

Variational Data Assimilation with Spatial and Temporal Observation Error Correlations of Doppler Radar Radial Winds

FUJITA Tadashi¹, SEKO Hiromu¹, KAWABATA Takuya¹, IKUTA Yasutaka¹,
SAWADA Ken¹, HOTTA Daisuke¹ and KUNII Masaru²

¹ Meteorological Research Institute, Japan Meteorological Agency, Tsukuba, Japan

² Numerical Prediction Division, Japan Meteorological Agency, Tokyo, Japan

e-mail: tfujita@mri-jma.go.jp

1. Introduction

High-frequency and high-resolution observations provide real-time detailed information of the atmospheric state, often related to high-impact severe weather events with small scale in time and space. In order to effectively utilize the dense observations in numerical weather prediction, it is important to appropriately handle the observation error correlation in data assimilation. This study investigates assimilation of Doppler radar radial winds, taking into account the spatial and temporal correlations of their observation errors in a variational data assimilation scheme.

2. Diagnosis of the Observation Error Correlation

The observation error correlation of Doppler radar radial winds is investigated by applying the method of Desroziers et al. (2005). The statistical samples are generated from a data assimilation cycle based on the previous version of the operational Meso-scale Analysis (MA; JMA 2019) of the Japan Meteorological Agency (JMA), replaced by the new version on 25 March 2020 (Ikuta et al. 2020). The previous MA ran a 3-hourly four-dimensional variational (4D-Var) scheme based on JNoVA (JMA Nonhydrostatic model-based Variational Data Assimilation; Honda et al. 2005), to produce the initial fields of the operational Meso-scale Model (MSM), an operational limited-area model with 5 km resolution.

The observation error correlation of Doppler radial winds from the Sapporo radar (43.14N, 141.01E) is diagnosed, based on the statistics of 1~8 Jul. 2018. During most of this period, a stationary front and a low pressure brought precipitation over this region, and Doppler radial wind data are continuously available (Fig. 1).

Figure 2 (a) displays the diagnosed correlation along the beam at the elevation angle of 1.1 deg. The half width of the correlation is about 10-20 km, increasing with distance from the radar site, consistent with Waller et al. (2016). The diagnosed temporal correlation (Fig. 2 (b)) has a half width of about 30-50 minutes, again showing an increase with the forecast time. The correlation thus looks to depend on beam propagation ranges, averaging cell volumes of radar observation (5 km x 5.625 deg.), beam widths and forecast time, suggesting contributions from representativeness and transformation errors involved with observation operator and forecast model.

3. Simple Variational Data Assimilation with Correlated Observation Error

A simple 2D-Var is used to investigate impact from incorporating correlated observation errors in data assimilation. The assimilation domain consists of 30 x 64 grid points in beam-range and azimuth-angle directions, corresponding to a resolution of 5 km x 5.625 deg. Innovations from the Sapporo radar are directory assimilated on the domain with a simple observation operator 1. The observation error correlations are approximated with Gaussian functions, with widths based on the statistics in the previous section.

Analysis increments (Fig. 3) show that including the correlation in observation errors (Fig. 3 (b)) helps to reflect detailed structures of the densely distributed innovations (Fig. 3 (a)) evenly over whole the domain, mitigating excessive increments in the case neglecting the correlation (Fig. 3 (c)) located where large innovations with identical sign are grouped (circled).

4. 4D-Var and Hybrid 4D-Var with Observation Error Correlated in Time and Space

Gaussian shaped observation error correlations are incorporated into the JNoVA 4D-Var, taking approximate spatial and temporal scales from the statistics. A hybrid 4D-Var with a flow-dependent background error is also implemented using ensemble perturbations from an EDA (Ensemble of Data Assimilations) consisting of six 4D-Var cycles with randomly perturbed observations. Doppler radar radial winds of 3 Jul. 2018 03~06 UTC from the Sapporo radar are assimilated with interval of 10 minutes using the 4D-Var and hybrid 4D-Var with assimilation windows of 3h to generate the analysis of 3 Jul. 2018 06UTC.

Figure 4 displays the time evolution of Doppler velocity increments along the beam at the azimuthal angle of 81.6 deg. (mostly east) and the elevation angle of 1.1 deg. A result from a simple variational method without temporal evolution operator is also shown for comparison. The simple variational method (b) gives increments well reflecting the innovation (a). However, the increment patterns stretch along the time axis, because the temporal evolution is not taken into account. In the 4D-Var (c), the temporal evolution operator works as an additional constraint to give increment patterns moving eastward with time, because the precipitation

area giving the Doppler velocities moves toward the east. The hybrid 4D-Var (d) reflects the eastward flow to the increment even from the early part of the assimilation window, because of the flow-dependent background error. This result suggests a high ability of the hybrid 4D-Var to extract information on the flow propagation from high-frequency observations.

Figure 5 displays RMSE against Doppler velocities from Sapporo and Kushiro (located about 280 km east of Sapporo) sites. For the hybrid 4D-Var, the results from 5 trials are shown, indicating uncertainties from the random perturbations added to the observations. The 4D-Var and hybrid 4D-Var both show main impact up to FT=6 (forecast time of 6 hours) for Sapporo (a) and up to FT=8 for Kushiro (b). The hybrid 4D-Var trials show a large diversity, but they give similar or smaller RMSEs compared to the 4D-Var for most of these periods of the experiments, suggesting a higher ability of the hybrid 4D-Var to obtain impact from the high-frequency observations. On the other hand, there are trials giving larger RMSEs than the 4D-Var for Kushiro (b) FT= -3~3, FT=9~11, and Sapporo (a) FT=6~9. This is because the times and locations not directly influenced by increments within the Sapporo observation range, which are far from the Sapporo site, might decrease the accuracy of the forecast. It is possible that there is some room for improvement in background error covariance from distant perturbations. It is one of the important

issues to investigate a sophisticated configuration of the ensemble to provide flow-dependencies for data assimilation.

Acknowledgements

This work was supported by JST AIP Grant Number JPMJCR19U2, JSPS KAKENHI Grant Number JP 19K23467, and “Advancement of Meteorological and Global Environmental Predictions Utilizing Observational ‘Big Data’ of the MEXT, Social and Scientific Priority Issues (Theme 4) to be Tackled by Using Post ‘K’ Computer” (hp180194, hp190156), Japan. This work is based on the operational NWP system developed by Numerical Prediction Division, Japan Meteorological Agency.

References

- Desroziers, G., et al., 2005: *Quart. J. Roy. Meteor. Soc.*, **131**, 3385–3396.
 Honda, Y., et al., 2005: *Quart. J. Roy. Meteor. Soc.*, **131**, 3465–3475.
 Ikuta, Y., et al., 2020: *CAS/JSC WGNE Res. Activ. Atmos. Oceanic Modell.*, **50**, 1–05.
 JMA, 2019: *Outline of the operational numerical weather prediction at the Japan Meteorological Agency. Japan Meteorological Agency*, Tokyo, Japan, 229 pp.
 Waller, J. A., et al., 2016: *Mon. Wea. Rev.*, **144**, 3533–3551.

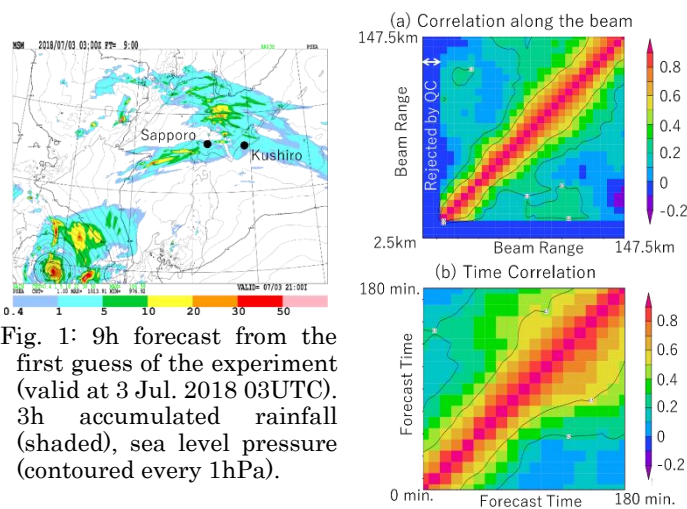


Fig. 1: 9h forecast from the first guess of the experiment (valid at 3 Jul. 2018 03UTC). 3h accumulated rainfall (shaded), sea level pressure (contoured every 1hPa).

Fig. 2: Observation error correlation of radial winds from the Sapporo Doppler radar. Statistic period is 1~8 Jul. 2018. Statistics of data at the elevation angle 1.1 deg. (a): correlation along the beam averaged over latter half of the 3h assimilation window. (b): temporal correlation averaged over beam range 47.5~97.5 km.

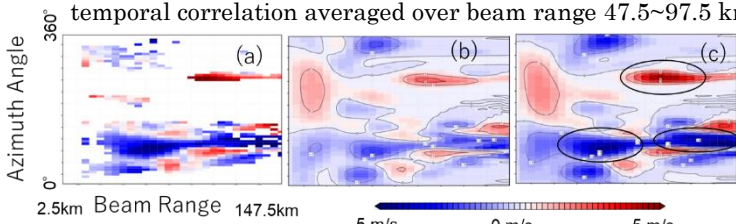


Fig. 3: Innovations and analysis increments from radial wind assimilation with the simple 2D-Var. (a) innovations, (b) increments with observation error correlations, (c) increments without observation error correlations.

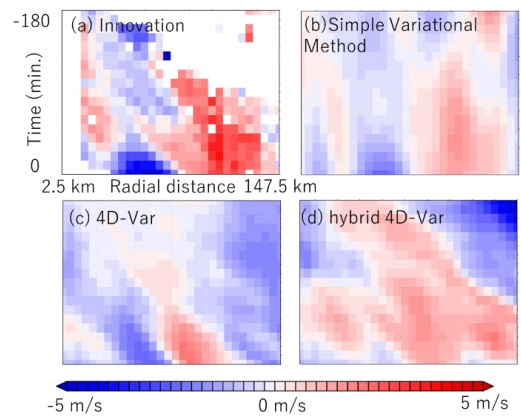


Fig. 4: Doppler velocity innovations and increments along the beam of the Sapporo radar at azimuthal angle 81.6 deg. and elevation angle 1.1 deg. Time evolution in the assimilation window (-180~0 min.).

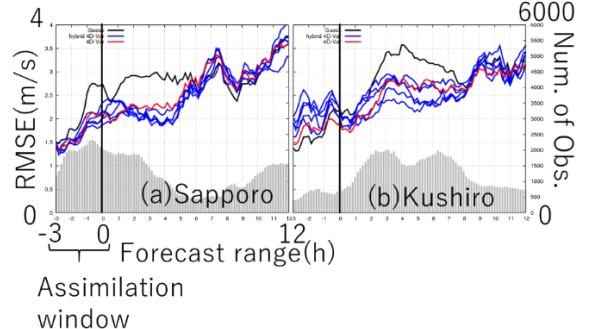


Fig. 5: RMSEs against Doppler velocity observations. (a) Sapporo radar, (b) Kushiro radar. Red: 4D-Var, Blue: 5 trials of the hybrid 4D-Var, Black: the first guess, Grey: number of observations (vertical axis on the right).